Available online at www.sciencedirect.com
ScienceDirect
C. R. Physique 9 (2008) 16–23
COMPTES RENDUS PHYSIQUE
http://france.elsevier.com/direct/COMREN/

New concepts for nanophotonics and nano-electronics

Propagation constants of guided waves in surface plasmon polariton gap waveguides excited through an I-shaped aperture

Kazuo Tanaka [a,*], Masahiro Tanaka [a], Kiyofumi Katayama [b], Daisuke Miyahara [a]

[a] *Department of Electronics and Computer Engineering, Gifu University, Yanagido 1-1, Gifu City, Japan 501-1193*
[b] *Faculty of Administration and Informatics, University of Hamamatsu, Hamamatsu City, Japan 431-2102*

Available online 20 February 2008

Abstract

The guided waves in the surface plasmon polariton gap waveguide (SPGW) excited by the Gaussian beam through the I-shaped aperture have been investigated by the three-dimensional simulations using a volume integral equation. Optical fields excited in the SPGW are investigated under practical conditions. The complex propagation constants are calculated from the simulated optical fields using the least-squares fitting. The dependence of the propagation constant, i.e., attenuation and phase constants, on the gap-width and on the gap-depth of SPGW is investigated. ***To cite this article: K. Tanaka et al., C. R. Physique 9 (2008).***

Résumé

Constantes de propagation des ondes guidées dans les guides optiques à fente à plasmon–polariton de surface excités à travers d'une ouverture en forme de I. Les ondes guidées dans un guide optiques à fente à plasmon–polariton de surface (SPGW) excité par un faisceau gaussien à travers un diaphragme en forme de I ont été étudiées au moyen de simulations tridimensionnelles basées sur une équation intégrale de volume. Les champs optiques excités dans un SPGW sont étudiés dans des conditions pratiques. Les constantes de propagation complexes sont calculées à partir des champs optiques simulés en utilisant une méthode des moindres carrés. La variation de la constante de propagation (c'est-à-dire des constantes d'atténuation et de déphasage) en fonction de la largeur de la fente et de sa profondeur est étudiée. ***Pour citer cet article : K. Tanaka et al., C. R. Physique 9 (2008).***

Keywords: Surface plasmon; Waveguide; Integral equation; Propagation constant

Mots-clés : Plasmon de surface ; Guide d'onde ; Guide optique ; Équation intégrale ; Constante de propagation

1. Introduction

Recently, the construction of optical circuits on nanometric scales has attracted much attention of many researchers in nanophotonics. It is not easy to construct optical devices whose size is much smaller than the optical wavelength and whose integration-density is much larger than that of the current optical integrated circuits due to the diffraction limit of light. The size of optical waveguide using surface plasmon polaritons (SPPs) can be significantly decreased as

* Corresponding author.
E-mail address: tanaka@tnk.info.gifu-u.ac.jp (K. Tanaka).

1631-0705/$ – see front matter
doi:10.1016/j.crhy.2007.10.010

compared to the conventional diffraction-limited optical waveguide [1–3]. So, the optical integrated circuit using SPPs is one of the promising candidates for future optical integrated circuits. Many interesting experimental or theoretical works that treat practical and concrete nanometric optical circuits using SPPs have been reported so far [4–9]. The guiding structure called SPP gap waveguide (SPGW) has been proposed by the authors [10–13]. The waveguide mechanism of the SPGW is derived from the low phase velocity exhibited by SPPs in nanometrically narrow gap-regions between two parallel metal substrates compared to that in wide gap regions. SPGWs have been demonstrated to guide, divide, and bend optical waves with acceptable losses in nanometric circuits.

In the design of optical circuits by using SPGW, one of the most fundamental and important parameters is the propagation constant of the guided waves. Since metals are dielectric objects with complex permittivity in the optical frequency region, the propagation constant of guided waves in the SPGW has complex value inevitably, i.e., attenuation constant and phase constant. The computations of complex propagation constants for the SPGWs and the similar structure have been performed by the finite-different time-domain (FDTD) method so far [14–16]. However, the investigation of guided waves in SPGW excited in the practical situation in not sufficient. The excitation of guided waves by practical techniques and propagation characteristics of excited guided-waves in SPGW will be important for experimental study of SPGW. Furthermore, numerical techniques of computation of propagation constants by the integral equation method will be also important, because the integral equation method is often used in simulation in nanophotonics.

In this article, we consider the experimental situation, i.e., the problem of the excitation of guided waves in SPGW of open type through an I-shaped aperture. We perform computer simulation of this 3D scattering problem by the volume integral equation. Then we calculate the complex propagation constants of the guided waves excited in the SPGW by least-squares fitting. The basic characteristics of optical intensity excited in the SPGW and dependence of propagation constants on the gap-width and gap-depth has been investigated.

2. Geometry of the problem

The geometry of the problem considered in this article is shown in Fig. 1. Two identical thick metallic (A_u) slabs whose size is given by $D \times d \times l$ are placed on the same plane parallel to the x–z plane with a gap-with w between two slabs, as shown in Fig. 1. The permittivity of the metallic slabs is assumed to be ε_1. In order to reduce the parameters of the problem, the surrounding space is assumed to be a free space whose permittivity is denoted by ε_0. The phase velocity of SPP in the gap region between two slabs is smaller than that in the surrounding free space when the gap-size is much smaller than the wavelength [10]. Hence, the optical field is confined in the gap region and is guided along the gap, i.e., the structure shown in Fig. 1 constitutes a straight SPGW. Guided waves in the SPGW can be excited through an I-shaped entrance aperture created in a rectangular thick metallic screen shown in Fig. 1. The size

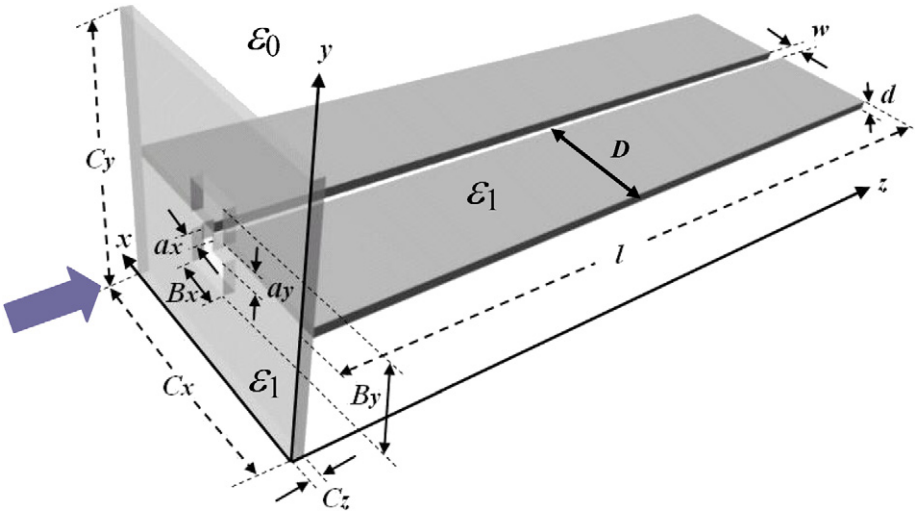

Fig. 1. Geometry of the problem used in the simulation.

of the rectangular screen is given by $C_x \times C_y \times C_z$ and is assumed to be $C_x = (2 \times D + w)$ in Fig. 1. The screen is made of same material (A_u) as that of metallic slabs and is placed on the plane parallel to the x–y plane as shown in Fig. 1. The center of the screen coincides with the center axis of the SPGW in Fig. 1.

The I-shaped entrance aperture consisting of a rectangular narrow gap-region of $a_x \times a_y$ sandwiched by two rectangular wide gap-regions of $B_x \times (B_y - a_y)/2$ as shown in Fig. 1. The I-shaped aperture in metallic screen is also a SPGW, and the SPP excited within is confined in the narrow-gap region in the aperture. Through this paper, we assume that $a_x = w$ and $a_y = d$ and call w and d the gap-with and gap-depth, respectively.

A Gaussian beam is set normally incident to the screen from the negative z direction in Fig. 1. The electric field polarization at $z = 0$ is set parallel to the x axis and the amplitude on the beam axis at $z = 0$ is unity. It is assumed that the beam axis coincides with the center axis of the SPGW. The spot size of the incident beam is set to be sufficiently smaller than the size of the metallic screen of size $C_x \times C_y$. So, the negligibly small guided wave is excited in the straight SPGW by the incident field diffracted by the screen.

3. 3D simulations by Volume Integral Equation

The scattering problem for the metallic structure shown in Fig. 1 is solved using a volume integral equation under the assumption of time dependence $\exp(+j\omega t)$, as given by

$$\boldsymbol{E}^i(\boldsymbol{x}) = \boldsymbol{D}(\boldsymbol{x})/\varepsilon_r(\boldsymbol{x}) - \left(k_0^2 + \nabla\nabla\cdot\right)\boldsymbol{A}(\boldsymbol{x}) \tag{1}$$

where $k_0 = \omega/c$ (c is light velocity in free space), $\boldsymbol{D}(\boldsymbol{x})$ is the total electric flux, $\boldsymbol{E}^i(\boldsymbol{x})$ is the incident electric field, and $\boldsymbol{A}(\boldsymbol{x})$ is the vector potential, which is expressed by the following volume integral [17,18]:

$$\boldsymbol{A}(\boldsymbol{x}) = (1/\varepsilon_0) \iiint_V \left\{\left[\varepsilon_r(\boldsymbol{x}') - \varepsilon_0\right]/\varepsilon_r(\boldsymbol{x}')\right\} G(\boldsymbol{x}|\boldsymbol{x}')\boldsymbol{D}(\boldsymbol{x}')\,\mathrm{d}v' \tag{2}$$

Here, $G(\boldsymbol{x}|\boldsymbol{x}')$ is a free-space Green's function given by

$$G(\boldsymbol{x}|\boldsymbol{x}') = \exp\left(-jk_0|\boldsymbol{x} - \boldsymbol{x}'|\right)/\left(4\pi|\boldsymbol{x} - \boldsymbol{x}'|\right) \tag{3}$$

The volume integral region V in (2) represents the entire space, and $\varepsilon_r(\boldsymbol{x})$ represents the distribution of permittivity, where $\varepsilon_r(\boldsymbol{x}) = \varepsilon_1$ in metal and $\varepsilon_r(\boldsymbol{x}) = \varepsilon_0$ in the surrounding free space of the SPGW and metallic screen. The expression of the incident Gaussian beam can be found in the literature [19]. To obtain the numerical solution, the entire region of the problem is divided into small discretized cubes of size $\delta \times \delta \times \delta$, and volume integral, Eq. (1) with (2), is discretized by the method of moments using roof-top functions as a basis and testing functions. The resultant system of linear equations is then solved by iteration using the generalized minimized residual method (GMRES) with fast Fourier transformation (FFT). As the numerical evaluation is long and extraneous, and it can be found in the literature [17,18,20], the details are omitted in this paper.

The operating wavelength considered in this analysis is $\lambda = 632.8$ nm and the metal that constitutes SPGW is assumed to be gold (A_u) with a relative permittivity of $\varepsilon_1/\varepsilon_0 = -13.2 - j1.08$. The spot size of the incident Gaussian beam at $z = 0$ is λ. The following parameters are used in the simulation shown in Fig. 1:

- size of the metallic screen used for the entrance aperture: $C_x = C_y = 1148$ nm, $C_z = 201$ nm;
- cross-section of entrance aperture: $B_x = 302$ nm, $B_y = 403$ nm, $a_x = w$ and $a_y = d$;
- length of SPGW: $l = 6244$ nm;
- size of the discretized cube: $\delta = 10$ nm.

The gap-width w, gap-depth d, and the size of small gap-region of the entrance aperture a_x and a_y are changed so that $a_x = w$ and $a_y = d$. Fig. 2 shows the distribution of total optical intensity $|\boldsymbol{E}|^2$ on the plane parallel to the x–z plane and located at a distance of 5 nm above the slab surface for the case of $w = a_x = 101$ nm and $d = a_y = 101$ nm. The intensity scale is normalized by the incident beam intensity at $z = 0$. The same optical intensity on the plane that contains the center axis of the SPGW and is parallel to the parallel to the y–z plane is shown in Fig. 3. Standing waves can be clearly seen to arise along the SPGW in Figs. 2 and 3. These results show that the guided wave is excited through the entrance I-shaped aperture effectively in Figs. 2 and 3.

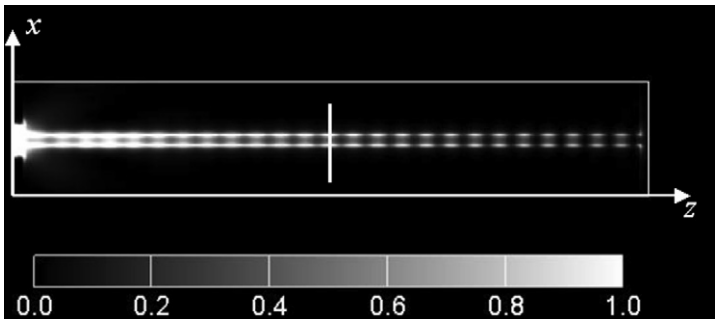

Fig. 2. Optical intensity $|\boldsymbol{E}|^2$ on a plane parallel to the x–z plane and located at a distance 5 nm above the slab surface for the case of $w = d = 101$ nm.

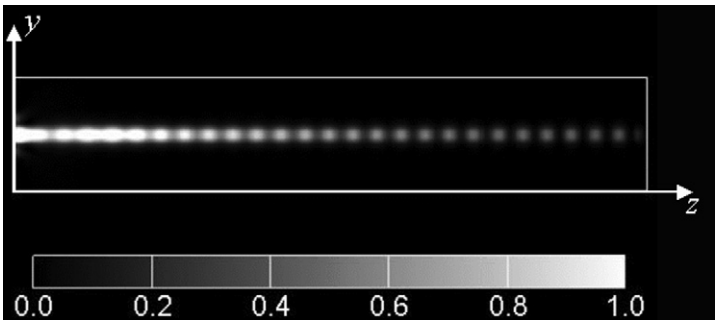

Fig. 3. Optical intensity $|\boldsymbol{E}|^2$ on a plane, which includes center axis of the waveguide and is parallel the y–z plane for the case of $w = d = 101$ nm.

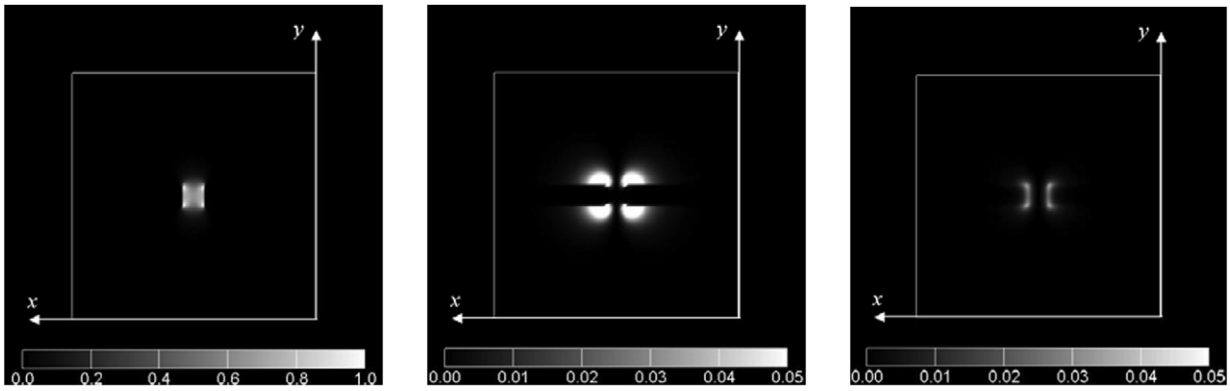

(a) (b) (c)

Fig. 4. Optical intensities of (a) $|E_x|^2$, (b) $|E_y|^2$ and (c) $|E_z|^2$ on a plane parallel to the x–y plane indicated by a white line in Fig. 2. Notice that the normalized intensity scales are (a) 0.0–1.0, (b) 0.0–0.05 and (c) 0.0–0.05.

Optical intensities of field components $|E_x|^2$, $|E_y|^2$ and $|E_z|^2$ on a plane parallel to the x–y plane indicated by a white line in Fig. 2 are shown in Fig. 4. The electric field of the guided wave excited in the SPGW is mainly composed of the x-component. From Figs. 2 to 4, the guided wave is confined in the gap-region in the SPGW and is guided along the SPGW.

The one-dimensional distributions of the optical intensities along a line parallel to the z-axis inside the SWPG are shown in Fig. 5. This line is located close to the side surface of the gap, i.e., concretely it is placed at coordinates of $x = D + 5$ nm and $y = C_y/2$, in Fig. 1, because the intensity on the center axis is smaller than that close to the surface of the gap. The results with a parameter gap-width w for the case of $d = 101$ nm and with a parameter gap-depth d for the case of $w = 101$ nm are shown in Fig. 5(a) and in (b), respectively. Most results in Fig. 5 show the monotonous decay of envelope of standing waves and show the monotonic oscillation along the propagation distance z in the range

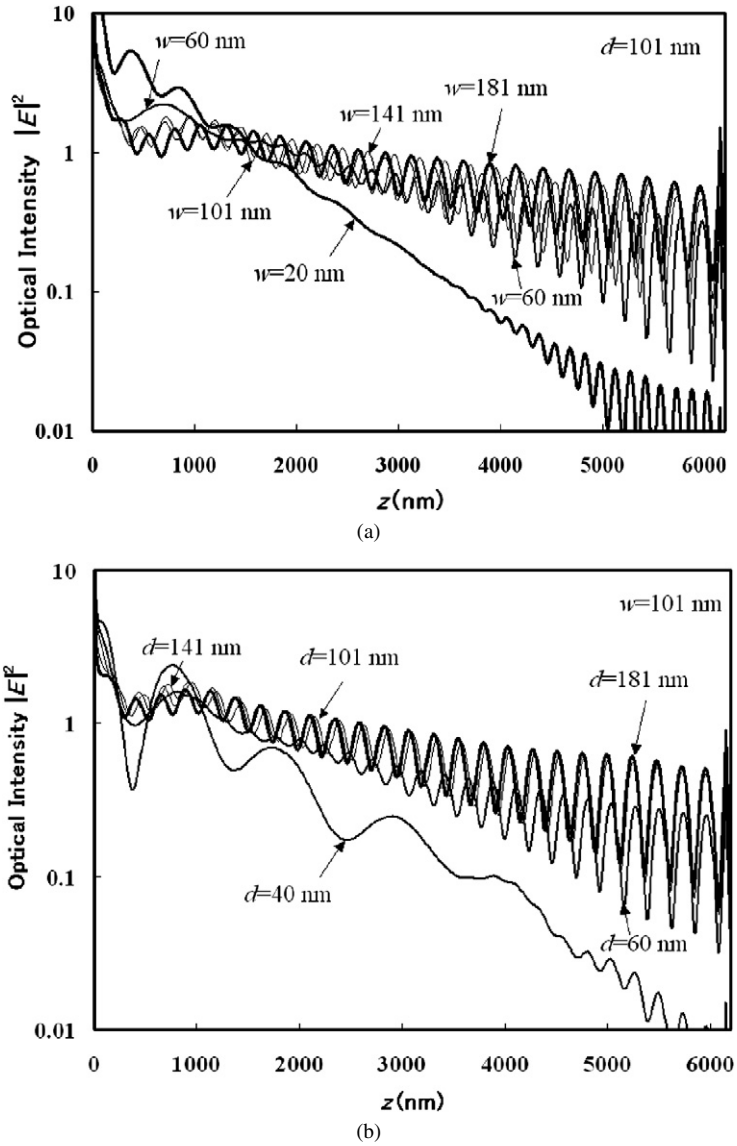

Fig. 5. Dependence of optical intensity $|\boldsymbol{E}|^2$ on propagation distance z in the SPGW with a parameter (a) gap-width w and (b) gap-depth d.

of 2000 nm $< z$. These characteristics show that two waves, which travel in opposite directions, have one propagation constant k_z in this range, i.e., a single-mode propagation. So, it is possible to calculate the single complex propagation constant k_z from the simulated optical fields.

In the range $z < 2000$ nm in Fig. 5, the interference between guided waves and other fields can be observed in the optical intensities. In order to know the origin of this interference, the optical intensities on the plane parallel to the x–z plane and located at a distance 5 nm above the slab surface for the cases of $w = 20$ nm, $d = 101$ nm and $w = 101$ nm, $d = 40$ nm are shown in Fig. 6(a) and (b), respectively. Both cases show rather large interferences in the optical intensity in Fig. 5. In Fig. 6, optical fields can be seen to extend widely near the entrance aperture. It is confirmed that the main component of these fields in Fig. 6 is the y-component.

So, these intensities represent SPPs excited on the surfaces of metallic slabs, which are parallel to the x–z plane, by the entrance aperture. Fig. 6 demonstrates that interference in Fig. 5 is due to the coupling between the guided waves and SPPs excited on the surfaces of the slabs. In particular, the coupling is strong for the case of $w = 101$ nm and $d = 40$ nm shown in Fig. 6(b).

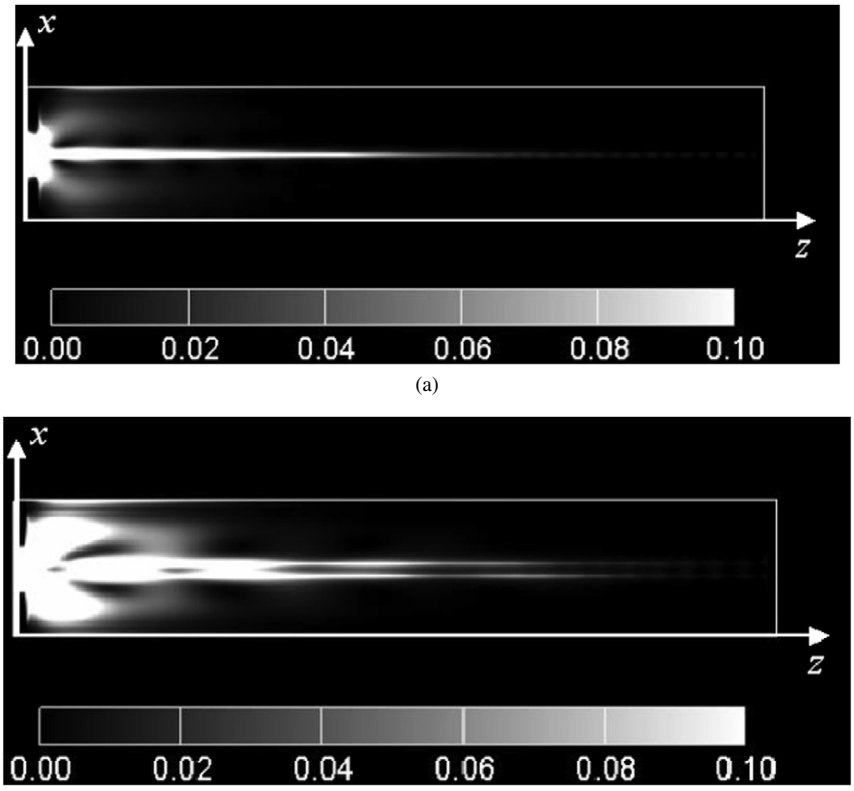

Fig. 6. Optical intensity $|\boldsymbol{E}|^2$ on a plane parallel to the x–z plane and located at a distance 5 nm above the slab surface for the cases of (a) $w = 20$ nm, $d = 101$ nm and (b) $w = 101$ nm, $d = 40$ nm. Notice that the normalized intensity scale is 0.0–0.1.

4. Computation of complex propagation constants by least-squares fitting

Let us consider the computation of the complex propagation constants defined by $jk_z = (\alpha + j\beta)k_0$ of the guided waves excited in the SPGW shown in Figs. 2–4, where α and β are the attenuation and phase constants normalized by the free space wavenumber k_0, respectively. When the attenuation constant α is rather large or the length l of the SPGW in Fig. 1 is sufficiently long in the simulation, the reflected guided wave from the end of the SPGW can be neglected because the excited guided wave will be negligibly small at the end of the SPGW due to the attenuation. In this case, it is easy to calculate k_z directly form simulation results as shown in Fig. 3. However, when the attenuation constant is not large and the sufficiently long SPGW cannot be used in the simulation, the reflected waves cannot be neglected. We consider the calculation of the complex propagation constants k_z from the field distributions as shown in Figs. 2–4.

In the region which is close to the entrance aperture and to the end of the SPGW shown in Fig. 1, we cannot consider that the field is the simple single-mode propagation from numerical examples shown in Fig. 5. However, in the limited range $Z_{\min} \leqslant z \leqslant Z_{\max}$ between the entrance and the end in the SPGW, it is possible to assume that the electric fields $e_i(z)$ $(i = x, y, z)$ along an appropriate given line parallel to the z-axis inside SPGW can be approximated by the following expression:

$$e_i(z) = A_i \exp\bigl[-(\alpha + j\beta)k_0 z\bigr] + B_i \exp\bigl[+(\alpha + j\beta)k_0 z\bigr] \quad (i = x, y, z) \tag{4}$$

where A_i and B_i $(i = x, y, z)$ are complex constants for x, y and z components of electric field, respectively. It is apparent that the first term in (4) represents the propagating wave to the positive z-direction and the second term represents the propagating wave to the negative z-direction in Fig. 1. The unknown constants A_i, B_i, α and β, can

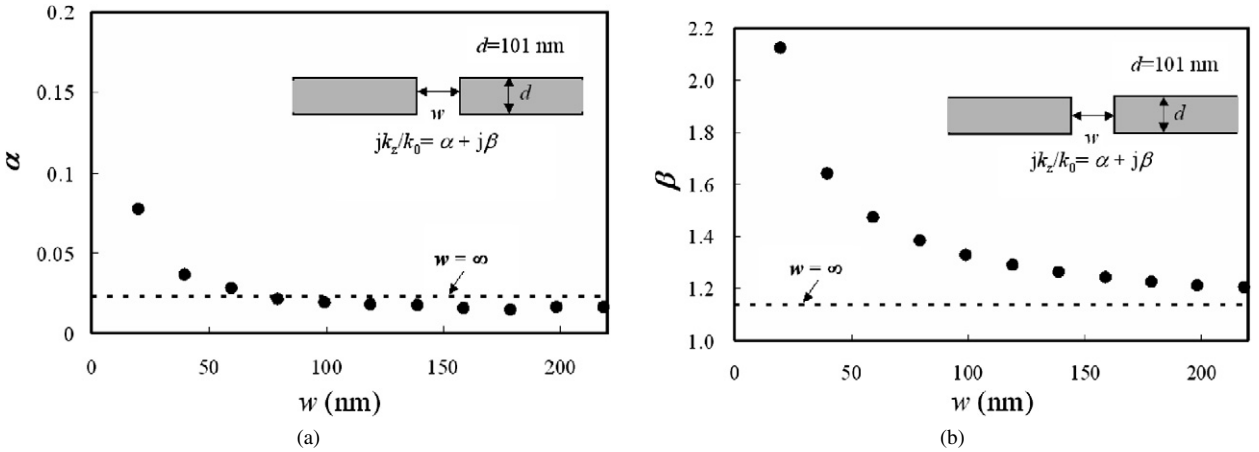

Fig. 7. Dependence of normalized (a) attenuation constant α, and (b) phase constant β on the gap width w for the case of $d = 101$ nm.

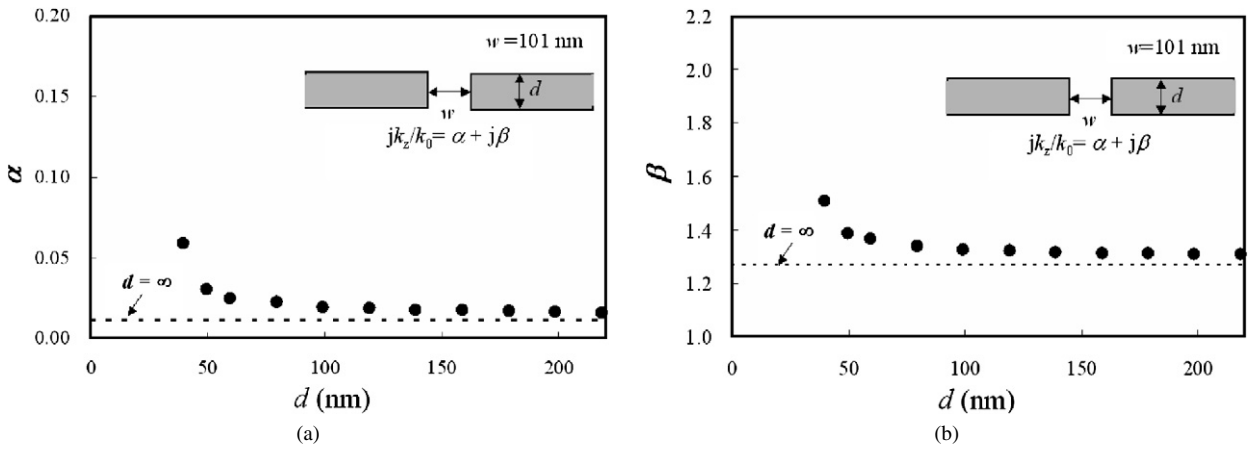

Fig. 8. Dependence of normalized (a) attenuation constant α, and (b) phase constant β on the gap height d for the case of $w = 101$ nm.

be approximately calculated so that the following least-squares errors at discrete points along the given line inside SPGW becomes minimum:

$$J(A_i, B_i, \alpha, \beta) = \sum_j \left| E_i(z_j) - e_i(z_j) \right|^2 \quad (i = x, y, z),\ Z_{\min} \leqslant z_j \leqslant Z_{\max} \tag{5}$$

where $E_i(z_j)$ represent the discrete value of the electric field components at discrete point z_i obtained by the numerical simulation. Parameters $Z_{\min}$ and $Z_{\max}$ are minimum and maximum values of the range where least-squares fitting is employed. The values of $Z_{\min} = 2014$ nm and $Z_{\max} = 6043$ nm are used in this paper from the results in Fig. 5. The propagation constants obtained are confirmed by comparing the electric fields obtained by the simulation with the reconstructed fields reconstructed by (4). It is confirmed that values of α and β do not depend on the electric field components and on the x and y coordinates of the line used in (5). We used x-component of electric field E_x in the calculation of (5), because E_y, E_z are much smaller than E_x as shown in Fig. 3.

The dependences of the attenuation constant α and phase constant β on the gap-width w for $d = 101$ nm and on the gap-depth d for $w = 101$ nm are shown in Figs. 7 and 8, respectively. Only for the case of the smallest gap-depth in Fig. 8, i.e., the case of $d = 40$ nm and $w = 101$ nm, the method based on (4) is not used in the calculation. In this case, the averaged values of α and β calculated from the field distribution in the range of 2014 nm $< z <$ 6043 nm are shown in Fig. 8. Both constants α and β decrease with the increase of gap-width w and they approach asymptotically to the results of $w = \infty$ as shown in Fig. 7. Results for the case of $w = \infty$ can be obtained by the simulation where one of the metallic slabs that constitute SPGW is eliminated in Fig. 1. It is possible to understand the existence of the

guided waves in this structure [21]. Under the conditions used in this paper, the dependence of α on the gap-width w is weak in the range of 60 nm $< w$ in Fig. 7. It is interesting that attenuation constants α are smaller than that of $w = \infty$ in the range of 80 nm $< w$ and there is the optimum gap-width w that gives smallest attenuation constant α of the guided waves in Fig. 7.

Both constants α and β also decrease with the increase of gap-depth d and they approach asymptotically to the results of $d = \infty$ as shown in Fig. 8. Results for the case of $d = \infty$ can be obtained easily because the problem becomes two-dimensional [10]. It is found that their dependence on the gap-depth d is weak for the case of 60 nm $< d$ in Fig. 8. In Fig. 8, the reason why α and β increase with the decrease of gap-depth d is that the guided wave shown in Figs. 2–4 is coupled to the SSP short-range mode excited in the metallic slabs [22].

5. Conclusions

The guided waves in the surface plasmon polariton gap waveguide (SPGW) excited by the Gaussian beam through the I-shaped aperture have been investigated by the three-dimensional simulations using a volume integral equation. Optical fields excited in the SPGW were calculated under practical conditions. The complex propagation constants are calculated from the optical fields using the least-squares fitting. The dependences of the attenuation and phase constants on the parameters of the waveguide were investigated. Parameters used in this paper are practical value for the experiment. Results obtained in this paper will be useful for the experimental study of SPGWs.

Acknowledgements

We would like to thank Prof. Frédérique de Fornel of University of Bourgogne for encouragement and help with the submission of this paper.

References

[1] J. Takahara, S. Yamagishi, H. Taki, A. Morimoto, T. Kobayashi, Opt. Lett. 22 (1997) 475–477.
[2] W.L. Bames, A. Dereux, T.W. Ebbesen, Nature 424 (2003) 824–830.
[3] S.I. Bozhevolnyi, V.S. Volkov, E. Devaux, T.W. Ebbesen, Phys. Rev. Lett. 95 (2005) 046802.
[4] L. Salomon, G. Bassou, H. Aourag, J.P. Dufour, F. de Fornel, F. Carcenac, A.V. Zayats, Phys. Rev. B 65 (2002) 125409.
[5] R. Charbonneau, P. Berini, E. Berolo, E. Lisicka-Shrzek, Opt. Lett. 25 (2000) 844–846.
[6] D.F.P. Pile, D.K. Gramotnev, Opt. Lett. 29 (2004) 1069–1071.
[7] D.K. Gramotnev, D.F.P. Pile, Appl. Phys. Lett. 85 (2004) 6323–6325.
[8] T. Goto, Y. Katagiri, H. Fukuda, H. Shinojima, Y. Nakano, I. Kobayashi, Y. Mitsuoka, Appl. Phys. Lett. 84 (2004) 852–854.
[9] H. Ditlbacher, J.R. Krenn, G. Schider, A. Leitner, F.R. Aussenegg, Appl. Phys. Lett. 81 (2002) 1753–1755.
[10] K. Tanaka, M. Tanaka, Appl. Phys. Lett. 82 (2003) 1158–1160.
[11] K. Tanaka, M. Tanaka, Jpn. J. Appl. Phys. 42 (2003) L585–L588.
[12] K. Tanaka, M. Tanaka, T. Sugiyama, Opt. Express 13 (2005) 256–266.
[13] K. Tanaka, M. Tanaka, T. Sugiyama, J. Light. Tech. 23 (2005) 3857–3863.
[14] L. Lui, Z. Han, S. He, Opt. Express 13 (2005) 6645–6650.
[15] B. Wang, G.P. Wang, Opt. Express 13 (2005) 10558–10563.
[16] D.F.P. Pile, T. Ogawa, D.K. Gramotnev, Y. Matsuzaki, K.C. Vernon, K. Yamaguchi, T. Okamoto, M. Haraguchi, M. Fukui, Appl. Phys. Lett. 87 (2005) 261114.
[17] E.K. Miller, L. Medgyesi-Mitschnag, E.H. Newsman (Eds.), Computational Electromagnetics Frequency-Domain Method of Moments, Institute of Electrical and Electronics Engineers Inc., 1992.
[18] P. Zwamborn, P.M. van den Berg, IEEE Trans. MTT 40 (1992) 1757–1766.
[19] G.S. Smith, An Introduction to Classical Electromagnetic Radiation, Cambridge University, New York, 1997.
[20] R. Barrett, M. Berry, T.F. Chan, J. Demmel, J. Donato, J. Dongarra, V. Eijkhout, R. Pozo, C. Romine, H. van der Vorst, Templates for the Solution of Linear Systems: Building Blocks for Iterative Methods, Society for Industrial and Applied Mathematics, 1994.
[21] D.F.P. Pile, T. Ogawa, D.K. Gramotnev, T. Okamoto, M. Haraguchi, M. Fukui, S. Matsuo, Appl. Phys. Lett. 87 (2005) 061106.
[22] J.J. Burk, G.I. Stegeman, T. Tamir, Phys. Rev. B 33 (1986) 5186–5201.